Biometals (2008) 21:189–196
DOI 10.1007/s10534-007-9107-6

Molecular modeling of zinc and copper binding with Alzheimer's amyloid β-peptide

Daxiong Han · Haiyan Wang · Pin Yang

Received: 19 August 2006 / Accepted: 26 June 2007 / Published online: 13 July 2007

Abstract Aggregation of the amyloid β-peptide (Aβ) into insoluble fibrils is a key pathological event in Alzheimer's disease. Cu(II) and Zn(II) ions were reported to be able to induce Aβ aggregation at nearly physiological concentrations in vitro. In this study, the binding modes of Cu(II) and Zn(II) in this process were explored by molecular modeling. In the pre-associated Aβ, Nτ atom of imidazole ring of His14, O atom of carbonyl of main-chain and two O atoms of water occupied the four ligand positions of the complex. While in the aggregated form of Aβ, the His13(N)–Metals–His14(N) bridges were formed through metal cross-linking action. These results would be helpful to put insight on revealing the formation mechanism of pathogenic Aβ aggregates in brain.

Keywords Molecular modeling · Amyloid β-peptide · Metal ions · Binding mode · Alzheimer's disease

D. Han (✉)
Department of Pharmacy, Medical College of Xiamen University, Xiamen 361005, China
e-mail: daxiong@xmu.edu.cn

H. Wang
Third Institute of Oceanography, State Oceanic Administration of China, Xiamen 361005, China

P. Yang
Institute of Molecular Science, Shanxi University, Taiyuan 030006, China

Introduction

Amyloid β-peptide (Aβ) is a natural peptide of about 39–42 amino acids, which can aggregate and accumulate to senile plaque (SP) cores. When these cores further co-localize with other numerous associated proteins and nonprotein components, neurotoxic SPs, a pathological character of Alzheimer's disease (AD) are thus formed (Hasegawa et al. 1999; Atwood et al. 2002; Storey and Cappai 1999). It has been reported that the imbalances of metal ions in brain may be related to the pathogenesis of AD. Microparticle-induced X-ray emission analysis has shown that Zn and Cu are significantly concentrated in the neurophil of AD patients and are further concentrated within the core and periphery of SPs (Lovell et al. 1998). Although the self-assembly process of Aβ has been observed in vitro to follow the nucleation-dependent growth in the absence of metal ions, the true mechanism of amyloid fibril formation remains obscure (Jarrett and Lansbury 1993; Padrick and Miranker 2002). Moreover, recent findings of Cu and Zn in the induction of significant Aβ aggregation at nearly physiological ion concentrations have received much attention in the study of molecular mechanism of Aβ aggregated form (Raffa and Gómez-Balderas 2005; Stellato et al. 2006; Dong et al. 2006). Circular dichroism spectroscopy, sedimentation assays and immobilized metal ion affinity chromatography show that rat Aβ (substitution of His13 by Arg) and histidine-modified human Aβ are not aggregated by

Zn(II) and Cu(II), indicating that histidine residues are essential for metal-mediated Aβ assembly (Liu et al. 1999; Atwood et al. 1998). However, no evidence reveals exact metal binding sites and models on Aβs (Zou et al. 2001; Luczkowski et al. 2002). In this study, we explored the possible binding modes of metal ions on Aβs in pre-associated Aβ complexes and insoluble aggregates by molecular modeling method under the assumption that the His13 and His14 of Aβs are the main ligands in the aggregation.

Simulation methods

Electron microscopic studies indicate that intact SP fibril cores are 40–80 Å in diameter, which are composed of two 20–40 Å filaments. The filaments are formed by aggregation of Aβ in repeat distances of 4.8 Å and 10.6 Å (Dong et al. 2003). These findings provide an experimentally constrained Aβ filament structure for theoretical model construction. It was also reported that metal coordinates mainly involves the Tyr10 and His at the amino acid positions 6, 13 and 14 of natural Aβ peptide respectively, among which His13 and His14 appear to be most critical for aggregation (Miura et al. 2000; Curtain et al. 2001). To increase the computational efficiency and emphasize the impact of these interactions on fibril formation, an experimentally reported Aβ variant (10–21) (amino acids 10–21 of natural Aβ) (Morgan et al. 2002), YEVHHQKLVFFA, was selected as a theory-model variant of Aβ(39–42). This Aβ(10–21) not only contains the His13 and His14 residues implicated in metal binding, but also keeps the overall amphiphilic distribution of amino acids, polar N-terminal and nonpolar C-terminal residues that exist in Aβ(39–42). Therefore, the Aβ (10–21) is a ideal model for Aβ aggregation modeling, which possesses the features and structures that might be presented in the SP cores.

It is assumed in our model that the fibrils are formed by three Aβ(10–21) strands aggregated into register β-sheets in parallel and anti-parallel modes, with a spacing of 5.0 Å between strands within a sheet. Four such sheets with the same secondary structure are laminated together, spaced by 10.0 Å, to be a rectangular fibril (Fig. 1). The side chains of the histidine residues at positions 13 and 14 are directed to opposite surfaces of the β-sheet, thus His13 and His14 residues from two neighbor sheets are proximal. This arrangement provides potential binding sites for chelating metal. In the cases of anti-parallel β-sheets, His13 and His14 residues along or between the sheets can combine to form a tetravalent site (Morgan et al. 2002).

It is challenging to simulate the interaction of transition metals with biochemical molecules by computational methods due to the complexity of electronic structure of these ions (multiple oxidation and coordinating states). An assumption that the metal binding works on the Aβ assembling directly is thus made to simplify the metal bridging function by using the simple coordination modes in metal-peptide complexes. As the consequence, the constraining function of metal on the conformations of both the metal-peptide complexes and the Aβ itself can be emphasized. Bonded approaches (Hou et al. 2001) and geometry optimization of molecular mechanics were used to reproduce geometries of Aβ(10–21) coordinated by metal ions. Such treatment (actual bonds) is helpful to fix metal ions at the site binding with designated ligand or in designated binding models. It is also favorable for comparing the relative stabilization of the Aβ structures among different binding modes. Several atoms are assigned to bind with metal ions, including the nitrogen atom (N) of the imidazole ring of His (Nτ), N of deprotonated amide of His (Nπ), the oxygen atom (O) of the carbonyl of main-chain, N of deprotonated amide of main-chain and O of water. The localization of these ligand atoms is illustrated in Fig. 2. Cu(II) and Zn(II) can bridge peptide chains through commonly-encountered tetrahedral coordination with the side chain residues of peptides. Regardless of the various valence coordinates actually adopted by metal ions, the number of ligand atoms coordinated to a metal ion by actual bond is fixed to four in our modeling process. Moreover, explicit consideration of the influence of water environment on the binding system is so extravagant that only limited water molecules are actually adopted to fill the metal valence. Most bond and angle parameterization associated with the Cu(II) and Zn(II) is derived from previous works (Hoops et al. 1991; Reichert et al. 2001). Other parameters are got following the default parameters scheme described in the appropriate manuals of Amber96 in Hyperchem6.0 (Hypercube Inc. 2000). In this study, all atoms are represented with the

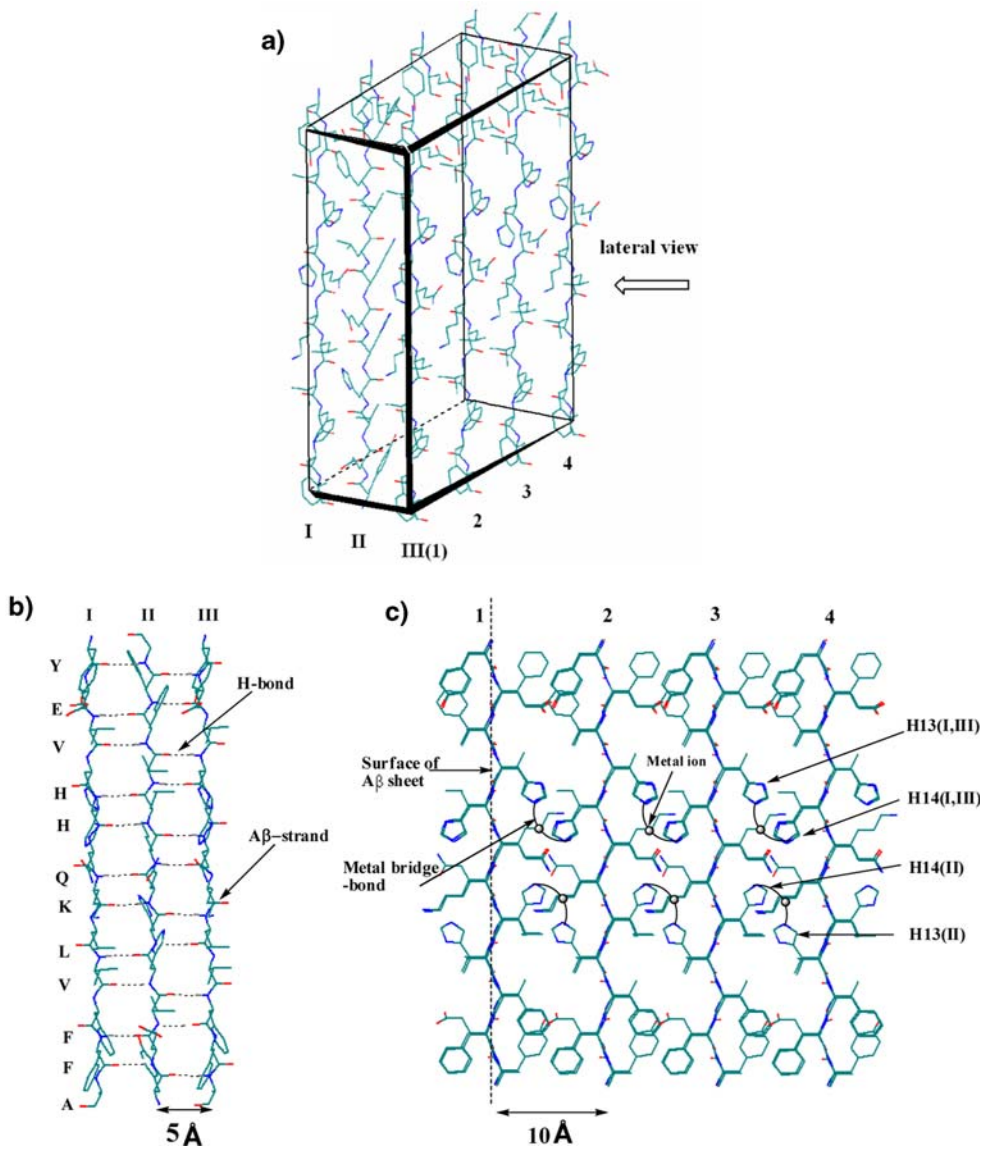

Fig. 1 (**a**) Structure of the fibril made up of anti-parallel Aβ(10–21) sheets; (**b**) amyloid β-sheet laying side-by-side (I, II and III represent strand numbering); (**c**) the lateral view of the β-sheets fibril (1, 2, 3 and 4 represent amyloid β-sheet lay numbering)

Fig. 2 The distribution of the ligand atoms which may coordinated to metal ions

atom types defined in the Amber96 force field and the related metal parameters are listed in Table 1.

In the state of pre-associated Aβ, the initial structure of the simple Aβ compounds, composed of an Aβ strand with one metal ion, is manually built by actual bonds as following: the metal ion is initialized at the geometry center of the related ligand atoms in the steric structure of a β-strand. These compounds are hydrated by a box of TIP3P water molecules. The optimum conformation of each compound is determined by comparing the energies of sample configurations from a molecular dynamics (MD) trajectory. The MD protocol contains an equilibration part lasting 5000 steps (1 step = 1 fs) and a sample part lasting 500 steps in water box at temperature of 298K. Each 100 steps is sampled for a configuration, and total five configurations of a compound are extracted from the water box. These five configurations are energy-minimized and the minimum one is chosen as the optimum configuration of the compound.

In the cases of complex Aβ compounds involving the interaction of multi-Aβ strands with one metal ion in the aggregated Aβ state, two types of Aβ fibrils, the parallel and anti-parallel β-sheet are chosen for metal binding modes analysis. In the Aβ(10–21) fibril the metal binding sites are repeatable, depicted as Fig. 1c. To focus on the impact of metal linking fashions on fibril formation, two/four strands for parallel/anti-parallel Aβ complexes (i.e., dimeric and four-meric Aβ complexes, Fig. 4) are extracted from the rectangular Aβ(10–21) fibril constructed previously (Fig. 1). For the parallel β-sheet, the His13 and His14 residues of I, II and III strands are each parallel to approach on the opposite surfaces of the β-sheet; whereas for the anti-parallel, the His13 and His14 residues of II strands are not proximal with those of I and III strands. The remarkable distinction of metal coordination environment leads to the different numbers of Aβ(10–21) strands selected to simulate the part Aβ fibril. Many possible linking fashions of the extracted multi-Aβ strands with a metal ion are built and energy minimized in the same way as the simulation of single Aβ strand case previously. The selected linking fashions, corresponding to lower potential energies, are then applied to the coordination of whole Aβ fibril.

All calculations are performed on a "DELL" workstation utilizing the Amber96 in Hyperchem6.0 (Hypercube Inc. 2000). Geometry optimization is carried out by the conjugate gradient minimizer with a convergence criterion of 0.1 kcal/mol per Å (assigning a dielectric constant of 4r).

Results and discussion

Binding mode of pre-associated Aβ

Before Aβ aggregate, there used to be an allosteric transition from α-helix to β-fold for soluble Aβ. Since a β-strand would be the key transitional structure of Aβ before aggregations, the interaction between metal ions and β-strands is studied to explore the soluble binding mode. In basis of systematic combination of the ligand atoms in Fig. 2, fifty possible binding sites and modes (data not shown) are evaluated to determine the optimum configurations of Cu(II)/Zn(II) binding to Aβ(10–21). Nτ of His14, O of peptide-bond in Val12 and two O atoms of water coordinate with Zn(II) to form the tetrahedron geometry of [3O,1N] (Fig. 3c), giving the lowest potential energy −27.76 kcal/mol (the potential energy of Aβ(10–21) peptide in the β-sheet structure is set to the reference value). Nτ of His14, O of peptide-bond in Glu11 and two O atoms of water coordinate with Cu(II) [3O,1N] (Fig. 3d), giving the lowest potential energy −6.21 kcal/mol. Miura suggested that in the soluble complex formed between Cu(II) and Aβ, the Nπ atom

Table 1 Force field parameters for Zn(II) and Cu(II) ions

Atom type	R* (Å)	Eps			
Zn	2.268	0.2000			
Cu	2.328	0.2000			
Bond	R_{eq} (Å)	Kr (kcal/Å^2)	Angle	θ_{eq} (degree)	K_θ (kcal/rad^2)
Zn–N	2.050	40.00	N–Zn–N	109.5	20.00
Zn–O	2.050	40.00	N–Zn–O	109.5	20.00
Cu–N	2.092	204.4	N–Cu–N	180.0	2.905
Cu–O	2.092	204.4	N–Cu–O	180.0	2.905

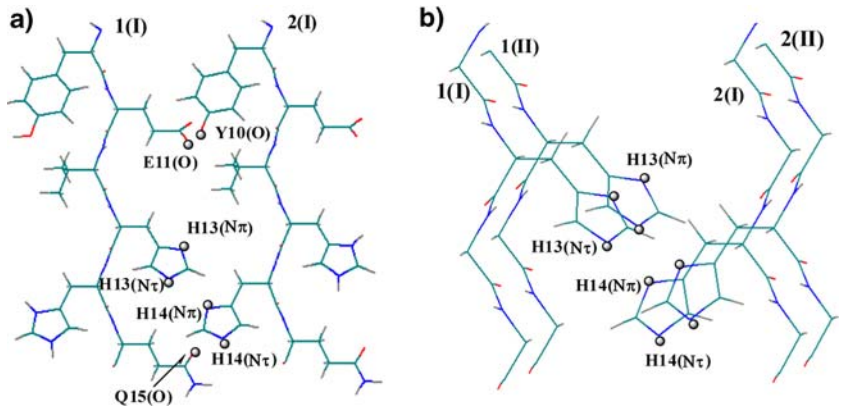

Fig. 4 Distribution and label of the atoms coordinating to metal ions in the part Aβ(10–21) fibril. (**a**) Anti-parallel fibril; (**b**) parallel fibril. I and II represent strand numbering; 1 and 2 represent amyloid β-sheet lay numbering

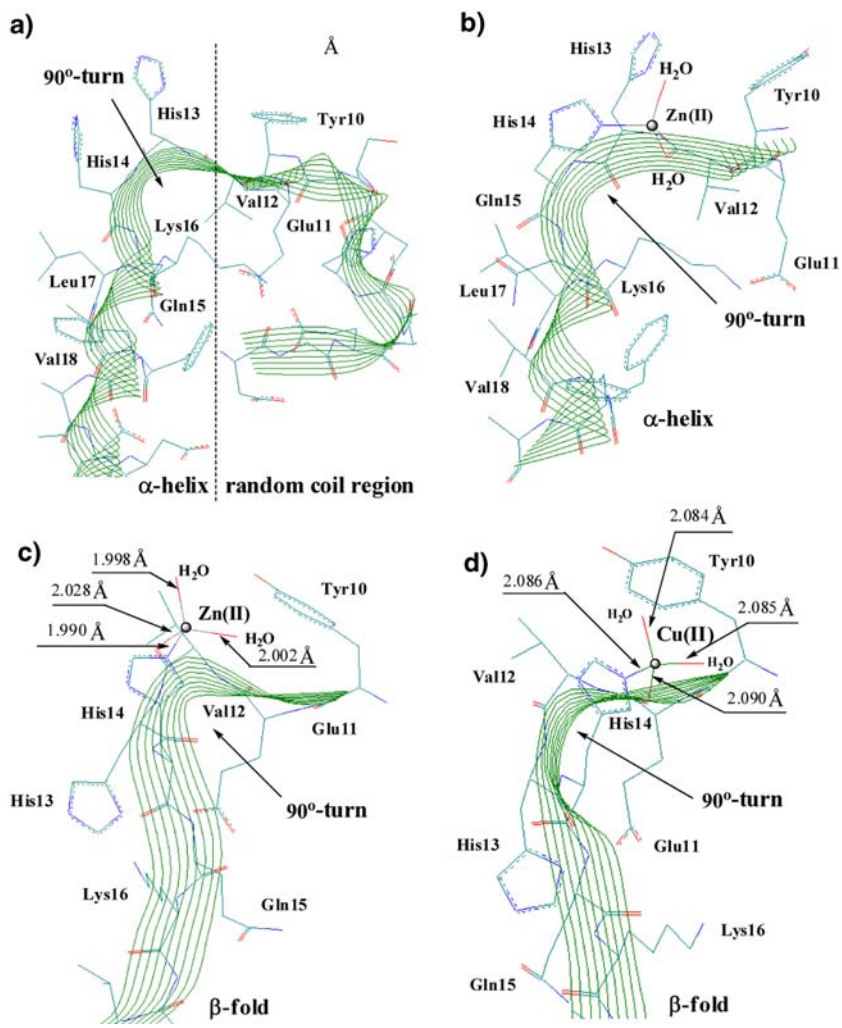

Fig. 3 (**a**) The soluble natural structure of the part Aβ(1–40); (**b**) the conformation of Zn(II) binding into the natural Aβ(10–21) by the [3O,1N] coordination; (**c**) the conformation of Zn(II) binding into the constructed Aβ(10–21) by the [3O,1N] coordination; (**d**) the conformation of Cu(II) binding into the constructed Aβ(10–21) by the [3O,1N] coordination. The ribbon represents the secondary structure

of a histidine residue together with two or three deprotonated amide nitrogens at the neighboring position could chelate a Cu(II) ion in a tetragonal geometry (Miura et al. 2000). However, our modeling results show that it is unfavorable to bind to Cu(II) or Zn(II) against the coordination linkage described by

Miura due to their high positive potential energy. When three or four neighboring atoms within an Aβ strand coordinate with a metal ion, the notable distortion of peptide β-structure is observed, accompanied with the remarkable increase of the bond straining and system potential. As results, it is suggested that two atoms at most from an Aβ strand are allowed to simultaneously coordinate with a metal ion by stronger coordinate bond.

A 90°-turn is found in the conformation of metal ions bounded Aβ(10–21) (Fig. 3c, d). This feature is dramatically similar to the soluble natural structure of Aβ(1–40) (Coles et al. 1998), as shown in Fig. 3a. Since the Aβ(10–21) is optimized by itself not to produce a 90°-turn, the metal binding may be responsible for the 90°-turn. Moreover, the binding of a Zn(II) ion to the Aβ(10–21) fragment extracted from natural Aβ(1–40) exhibit the same binding mode of [3O,1N] as the constructed Aβ(10–21) variant (Fig. 3b). The potential energy of the natural Aβ(10–21) bound by Zn(II) (−19.00 kcal/mol) is just slightly more negative than that of before binding (−17.80 kcal/mol), and the whole conformation of the natural Aβ(10–21) hardly changes before and after the Zn(II) binding (Fig. 3a and b). This implies that the 90°-turn region of the natural Aβ(1–40) might be a good site for Zn(II) binding, and the binding might be a reversible process. Furthermore, the Aβ(10–21) potential energy of α-helical structure, α-helix with Zn(II) binding (Fig. 3b) and β-fold with Zn(II) binding (Fig. 3c) obviously decrease gradually from −17.80 to −19.00 to −27.76 kcal/mol. It hints that the Zn(II) interaction with N terminus of Aβ may be responsible for inducing or enhancing the β-fold conformation. It can be further inferred that the complexation of Aβ with Zn(II) play as a conformational switch, which triggers the conformational transition between α-helix and β-sheet. Different from Zn(II) binding, the Aβ(10–21) potential energy of α-helical structure, α-helix with Cu(II) binding and β-fold with Cu(II) binding (Fig. 3d) are −17.80, −10.84 and −12.06 kcal/mol, respectively. It indicates that the structural basis for Cu(II) binding and the allosteric basis for cooperativity may be mediated by the β-sheet conformations. In other words, only the Aβ conformations contain mainly β-sheet, could Cu(II) have higher affinity for Aβ and accelerate Aβ to associate.

Solvent pH is a key factor in controlling the coordination between Aβs and metal ions. Under certain pH environment, the metal ions can coordinate with the Aβs. The metal ion affinity abilities determine the effects of Zn(II) and Cu(II) in the induced aggregation. The stronger affinity ability the metal ion own, the shorter the binding bond lengths and the stronger the drawing force of the metal ions bind to the Aβ residues. The drawing force can induce the changes in the peptide secondary structure. Through observing the changes of potential energy, we find that Zn(II) can induce Aβ to aggregate in β-sheet and α-helical conformations, while Cu(II) can only induce β-sheet aggregation form. Figure 3c, d shows that the bond lengths of Nτ(His14)-Zn(II) (1.990 Å), O(Val12)–Zn(II) (2.028 Å) and O(water)–Zn(II) (1.998 Å and 2.002 Å)are shorter than those of Nτ(His14)–Cu(II) (2.086 Å), O(Glu11)–Cu(II) (2.090 Å) and O(water)–Cu(II) (2.084 Å and 2.085 Å) respectively. These results indicate that Zn(II) binding makes the coordination residues closer, thus leads to more obvious changes in peptide conformation than Cu(II) binding. The results of low affinity for Cu(II) binding and high affinity for Zn(II) binding are well consistent with earlier report (Atwood et al. 1998). While solvent pH promotes the α-helical conformation, the Aβ aggregation by Cu(II) is rapidly abolished, but Zn(II)-induced Aβ aggregation shows much more resistant to pH at similar conditions. Therefore, α-helical conformation may be unfavorable for the Cu(II) coordination that mediates peptide assembly(Atwood et al. 1998).

Binding mode of aggregated Aβ

Some experiments have reported the presence of covalently crosslinked dimeric and trimeric Aβ species with metal ions in neuritic plaque (Roher et al. 1996). According to this fact, a possible mechanism on Aβ from soluble phase to fibril would be simulated by the crosslink model with metal ions. It has been characterized that the secondary structure of synthetic Aβ fibril is a repeating, parallel or anti-parallel, β-pleated sheet structure. However, up to now, there is no direct evidence for the configuration of Aβ fibril within SPs (Zou et al. 2001; Luczkowski et al. 2002; Dong et al. 2003). Therefore, two types of Aβ fibril (parallel and anti-parallel β-sheet) are investigated for their metal binding modes in the study. The potential energy of the

Aβ fibril with different metal-bridge bonds are listed in Table 2, and illustrated in Fig. 4.

As indicated in Table 2, the anti-parallel Aβ fibril gives the minimum potential energy of −405.02 kcal/mol. This is subject to the Zn(II) optimum binding mode that His13(Nτ), His14(Nτ) and 2Wat(O) atoms form the tetrahedron conformation. The graphics corresponding to the optimum binding mode (Fig. 1c), illustrates that the His13(Nτ)–Zn(II)–His14(Nτ) bridges formed by Zn(II) cross-linking action may be an intrinsic force to transform Aβ from soluble phase to fibril phase. This finding is in well agreed with Miura's deduction from the Raman spectra (Miura et al. 2000). The effects of Zn(II) binding were observed by histidine Raman bands. Upon the binding of Zn(II), the 1570 cm^{-1} band of metal-free histidine was diminished in the spectrum of insoluble aggregates, and concomitantly a band at 1604 cm^{-1} gained intensity. The peak at 1604 cm^{-1} could be assigned as Zn(II) binding to the Nτ atom of histidine in the insoluble Zn(II)–Aβ(1–40) complex. In the view of theoretical computation, the more negative of potential energy, the more stable of binding composite. Though Cu(II) displays similar role as Zn(II) in Aβ binding, its capability of inducing Aβ assembly is markedly weaker than Zn(II). The bridge formation leads to the system potential energy dropping rapidly from −36.40 (without metal) to −405.02 kcal/mol (Zn(II) binding) and −281.38 kcal/mol (Cu(II) binding). Accordingly, it stabilizes the structure of the constructed SP core. It indicates that metal ions not only play an important role in maintaining the structural integrity of the Aβ aggregated form, but also provide a seed for the formation of amyloid steric structure, i.e. Aβ strands in a β-sheet are linked by intermolecular H-bond and Aβ strands among β-sheet are linked by metal-bridge bond (Fig. 1). In the case of the same metal binding modes the potential energy of the anti-parallel Aβ fibril is obviously lower than that of parallel. Consequently, it can be explained as follows: (1) the difference in secondary structure of Aβ fibril itself determines the different potential energy. Without metal binding, the potential difference between anti-parallel and parallel for the Aβ(10–21) fibril is −36.40 kcal/mol (the potential energy of anti-parallel is more negative); (2) the metal-bridge bonds in I, II and III strands of parallel structural locate in a plane, which goes against stabilizing the binding system due to the overwhelming concentration of positive charge injected by metal ions. Therefore, it can be deduced that an anti-parallel rather than a parallel β-sheet is favorable for Aβ aggregated form.

To sum up, in this study the detailed information of Cu(II) and Zn(II) binding modes in Aβ fibril are investigated by theoretical simulation approach. It is depicted that the process of the Aβ aggregated form induced by metal ions might be present in the SPs. These results would provide potentially useful information for the pathological and biochemical studies. In particular, regardless of single Aβ strand or multi-strands within Aβ fibril, the metal-His(Nτ) ligation is the common feature that can effectively decrease the potential energy. It may be reasonable to deduce that the breakage of the metal-His(Nτ) bond might lead to the recovery of the peptide solubility. However, from the mechanism of Aβ aggregation presented here, it is clear that there is a theoretical thermodynamic basis for exploring metal binding modes. It is so

Table 2 Potential energies of the Aβ fibril with metal-bridge bond among Aβ sheets (kcal/mol)[a]

Ligand atom	Anti-parallel Aβ fibril		Parallel Aβ fibril	
	Cu(II)	Zn(II)	Cu(II)	Zn(II)
H13Nτ[1(I)], H14Nτ[2(I)], 2Wat(O)	−236.41	−405.02	−198.78	−327.49
H13Nπ[1(I)], H14Nπ[2(I)], 2Wat(O)	−279.05	−363.62	−183.32	−288.38
H13Nτ[1(I)], H14Nπ[2(I)], 2Wat(O)	−281.38	−367.50	−210.47	−301.06
Q15O[1(I)], H14Nτ[2(I)], 2Wat(O)	−233.52	−361.46	−181.22	−292.59
H13Nπ[1(I)], H13Nτ[1(II)], H14Nπ[2(I)], Wat(O)	−183.17	−232.75	−133.67	−180.75
H13Nτ[1(II)], H14Nπ[2(I)], 2Wat(O)	−132.70	No convergence	−86.24	−192.61
H13Nτ [1(II)], H14Nπ[2(I)], 2Wat(O)	−167.31	−254.56	−129.99	No convergence
H13Nτ [1(I)], H14Nπ[2(I)] H14Nτ [2(II)], Wat(O)	No convergence	−255.39	No convergence	−179.72

[a] The potential of the parallel Aβ fibril is regarded as reference value

expected that further experimental study may provide additional data to support such work.

Acknowledgments The authors acknowledge the support of the Science Foundation of Xiamen University (No. Z03120), the Grand Research Foundation of Fujian Province of China (No. 2005YZ1014) and the Natural Science Foundation of Fujian Province of China (No. 2006J0184).

References

Atwood CS, Martins RN, Smith MA, Perry G (2002) Senile plaque composition and posttranslational modification of amyloid-β peptide and associated proteins. Peptides 23:1343–1350

Atwood CS, Moir RD, Huang X et al (1998) Dramatic aggregation of Alzheimer Aβ by Cu(II) is induced by conditions representing physiological acidosis. J Biol Chem 273:12817–12826

Coles M, Bicknell W, Watson AA et al (1998) Solution structure of amyloid beta-peptide(1–40) in a water-micelle environment. Is the membrance-spanning domain where we think it is? Biochemistry 37:11064–11077

Curtain CC, Ali F, Volitakis L et al (2001) Alzheimer's disease amyloidbeta binds copper and zinc to generate an allosterically ardered membrane penetrating structure containing superoxide dismutase-like subunits. J Biol Chem 276:20466–20473

Dong J, Atwood CS, Anderson VE, Siedlak SL, Smith MA, Perry G, Carey PR. (2003) Metal binding and oxidation of Amyloid β within isolated senile plaque cores: raman microscopic evidence. Biochemistry 42:2768–2773

Dong J, Shokes JE, Scott RA, Lynn DG (2006) Modulating amyloid self-assembly and fibril morphology with Zn(II). J Am Chem Soc 128:3540–3542

Hasegawa K, Yamaguchi I, Omata S, Gejyo F, Naiki H (1999) Interaction between Aβ(1–42) and Aβ(1–40) in Alzheimer's β-Amyloid fibril formation in vitro. Biochemistry 38:15514–15521

Hoops SC, Anderson KW, Merz KM (1991) Force field design for metalloproteins. J Am Chem Soc 113:8262–8270

Hou TJ, Zhang W, Xu XJ (2001) Binding affinities for a series of selective inhibitors of gelatinase—a using molecular dynamics with a linear interaction energy approach. J Phys Chem B 105:5304–5315

HyperChem Release 6.0. Hypercube Inc. 2000

Jarrett JT, Lansbury PT (1993) Seeding "one-dimensional crystallization" of amyloid: a pathogenic mechanism in Alzheimer's disease and scrapie? Cell 73:1055–1058

Liu ST, Howlett G, Barrow CJ et al (1999) Histidine-13 is a crucial residue in the zinc ion-induced aggregation of the Aβ peptide of Alzheimer's disease. Biochemistry 38:9373–9378

Lovell MA, Robertson JD, Campbell JL, Markesbery WR 1998 Copper, iron and zinc in Alzheimer's disease senile plaques. J Neurol Sci 158:47–52

Luczkowski M, Wisniewska K, Kozlowski H, et al (2002) Specific binding of Cu2+ ions by a pentapeptide fragment present in the cysteine-rich region of amyloid precursor protein. J Chem Soc Dalton Trans 2266–2268

Miura T, Suzuki K, Kohata N, Takeuchi H (2000) Metal binding modes of Alzheimer's amyloid β-peptide in insoluble aggregates and soluble complexes. Biochemistry 39:7024–7031

Morgan DM, Dong JJ, Jacob J, Lu K, Apkarian RP, Thiyagarajan P, Lynn DG (2002) Metal switch for amyloid formation: insight into the structure of the nucleus. J Am Chem Soc 124:12644–12645

Padrick SB, Miranker AD (2002) Islet amyloid: phase partitioning and secondary nucleation are central to the mechanism of fibrillogenesis. Biochemistry 41:4694–4703

Raffa DF, Gómez-Balderas R et al (2005) Ab initio model studies of copper binding to peptides containing a His–His sequence: relevance to the β-amyloid peptide of Alzheimer's disease. J Biol Inorg Chem 10:887–902

Reichert DE, Norrby P, Welch MJ (2001) Molecular modeling of bifunctional chelate peptide conjugates. 1.Copper and indium parameters for Amber force field. Inorg Chem 40:5223–5230

Roher AE, Chaney MO, Kuo YM et al (1996) Morphology and toxicity of Aβ(1–42) dimmer derived from neuritic and vascular amyloid deposits of Alzheimer's disease. J Biol Chem 271:20631–20635

Stellato F, Menestrina G, Serra MD et al (2006) Metal binding in amyloid β-peptides shows intra- and inter-peptide coordination modes. Eur Biophys J 35:340–351

Storey E, Cappai R (1999) The amyloid precursor protein of Alzheimer's disease and the Aβ peptide. Neuropathol Appl Neurobiol 25:81–97

Zou J, Kajita K, Sugimoto N (2001) Cu inhibits the aggregation of amyloid β-peptide(1–42) in vitro. Angew Chem Int Ed 40:2274–2277